



An improved water correction function for Picarro greenhouse gas analyzers

Friedemann Reum¹, Christoph Gerbig¹, Jost V. Lavric¹, Chris W. Rella² and Mathias Göckede¹

¹Max Planck Institute for Biogeochemistry, Jena, Germany

5 ²Picarro Inc., Santa Clara, CA, USA

Correspondence to: Friedemann Reum (freum@bgc-jena.mpg.de)

Abstract. Measurements of dry air mole fractions of atmospheric greenhouse gases are widely used in inverse models of atmospheric tracer transport to quantify the sources and sinks of the gases. The measurements have to be calibrated to a common scale to avoid bias in the inferred fluxes. The World Meteorological Organization (WMO) has set requirements for the inter-laboratory compatibility of atmospheric greenhouse gas measurements to ± 0.1 ppm for CO₂ (Southern hemisphere ± 0.05 ppm) and to ± 2 ppb for CH₄. An established series of devices for measurements of greenhouse gas (GHG) mole fractions are the trace gas analyzers manufactured by Picarro, Inc. These have been shown to deliver dry air mole fractions with accuracies within the WMO goals when trace gas signals are measured in wet air and the effects of water vapor are corrected for. Here, we report for the first time on sensitivity of the pressure inside the measurement cavity of Picarro GHG analyzers to water vapor. This sensitivity induces biases in the inferred dry air mole fractions of CO₂ and CH₄ if they are obtained using the traditional water correction function. To correct for the pressure effect, we add a pressure-related term to the traditional water correction function, and consider differences between the traditional and enhanced water correction function to be biases of the traditional model. The effect primarily affects low water vapor mole fractions from about 0.05 to about 0.5 %, a domain that has gone undersampled in previous studies of the water correction for Picarro GHG analyzers. We observed biases up to about 40 % of the WMO tolerances (80 % for CO₂ in the southern hemisphere). The magnitude of the effect varied across instruments and appeared to be negligible for some, and our experimental results were more robust for CH₄ than for CO₂. Thus, correction coefficients should be determined for each analyzer individually. Applying our enhanced water correction function improves the accuracy of measurements of dry air mole fractions of CO₂ and CH₄ in humid air with Picarro GHG analyzers on a scale important for keeping the measurement accuracy within the WMO requirements.

1 Introduction

Measurements of atmospheric GHG mole fractions are integral data for quantifying the sources and sinks of the gases using inverse models of atmospheric transport (e.g. Kirschke et al., 2013; McGuire et al., 2012). Inverse models require atmospheric measurements calibrated to a common scale, because relative biases in the mole fraction data lead to biases in



the inferred fluxes. The World Meteorological Organization (WMO) has set compatibility goals for atmospheric CO₂ and CH₄ measurements to ± 0.1 ppm for CO₂ (± 0.05 ppm in the southern hemisphere) and ± 2 ppb for CH₄ (WMO, 2016).

In models of atmospheric greenhouse gas transport, the relevant atmospheric information is the dry air mole fraction, i.e. the number of molecules of the target gas divided by the number of air molecules, not including water vapor. Water vapor is excluded because its large variability would cover any signal in the trace gases. To measure dry air mole fractions in the humid atmosphere, there are two strategies: (i) drying the air before measurement and (ii) measuring the wet air signal and correcting for the effects of water vapor later. There are a variety of techniques to dry sample air, including cooling or streaming it through a nafion membrane dryer. Limitations of this strategy include maintenance requirements, minimum limits to the achievable dryness, and possibly effects of drying on the GHG mole fractions (Rella et al., 2013).

GHG analyzers manufactured by Picarro Inc. (Santa Clara, CA), which are based on the cavity ring-down spectroscopy technique (Crosson, 2008), are used at many sites of the international GHG monitoring network because of their signal stability. When using these instruments, the practice is often not to dry the sample air, but instead to measure wet air mole fractions and subsequently correct for the effects of water vapor. Cavity ring-down spectroscopy is based on absorption of laser light by the target gas inside a resonator cavity. Active temperature and pressure control in the cavity are built-in to establish the stable measurement conditions necessary for fitting absorption line shapes. To obtain dry air mole fractions, a water correction function is applied to CO₂ and CH₄ signals measured in wet air. The established form of the water correction function accounts for the dilution effect of water vapor and its effects on the shapes of the absorption lines (Chen et al., 2010; Rella et al., 2013). Dilution changes the target gas mole fraction linearly, and the effects of line shape changes on the mole fraction measurements are modeled as a second-degree Taylor series. Thus, the overall shape of the traditional water correction function is a parabola (with a dominant linear term and a small quadratic correction), by which measured wet air mole fractions are divided to obtain dry air mole fractions. By using these functions, water vapor effects on CO₂ and CH₄ can be corrected with residuals below the WMO goals. Better accuracy is achieved by determining individual coefficients for the water correction function specific to each analyzer (Chen et al., 2010; Rella et al., 2013).

Here, we report systematic biases of dry air mole fractions inferred using the traditional parabolic water correction functions that, to our knowledge, have not been investigated yet. In some cases, the observed systematic deviations were as high as about 40 % of the WMO tolerances (80 % for CO₂ in the southern hemisphere). The largest deviations were at low H₂O mole fractions around from about 0.05 to about 0.5 %. We found that only few measurement points at such low water vapor mole fractions were sampled in previous studies (Chen et al., 2010; Nara et al., 2012; Rella et al., 2013; Winderlich et al., 2010). In this study, we address the systematic deviations introduced by the traditional water correction function, and find that they can be explained by a dependency of the pressure inside the measurement cavity on the water vapor content in the sample air. We present a method to correct for the pressure effect, and quantify the impact this correction has on observations from the field.



2 Methods

2.1 Experiments

To determine the effect of water vapor on CO₂ and CH₄ measurements, dry air from pressurized gas tanks was humidified and measured with a Picarro GHG analyzer. Pressure in the measurement cavity of the analyzer was monitored with both the built-in internal pressure sensor and an additional external pressure sensor (Fig. 1).

To humidify the air stream, two different methods were used. The first approach was designed to allow stable maintenance of defined levels of the water vapor content. The dry air stream was split into two lines, one of which remained untreated. Air in the other line was directed through a gas washing bottle (glass) containing deionized water (depending on bottle size, about 15 ml to about 500 ml were used in the experiments presented here). Thus, air in this line was saturated with water vapor (mole fraction about 3 %). Subsequently, the two lines were joined again. The water vapor mole fraction in the re-joined line was controlled by adjusting the flow through the wet and dry lines using needle valves. For one of the experiments (Picarro #1, see Table 1), instead of using the gas washing bottle approach, air was humidified by mixing air from the gas tank and ambient laboratory air. From this experiment, only pressure data were analyzed.

The second humidification approach was the droplet method. For these experiments, the humidification unit described above was replaced with a tee piece. To humidify the air, a droplet of deionized water (~ 1 ml) was injected into the line through the tee piece using a syringe. Gradual evaporation of this water droplet then caused a gradient over time from high to low water vapor levels in the sample air.

Pressure inside the measurement cavity of Picarro GHG analyzers is kept stable by a feedback loop between a pressure sensor (General Electric NPC-1210) that is mounted inside the cavity, and the outlet valve of the cavity (inlet valve in so-called Flight-ready Picarro GHG analyzers, which are customized for airborne measurements). With this loop, the cavity pressure is kept stable at 140 Torr. Since Picarro reports cavity pressure in Torr, we will use this unit throughout this paper (1 Torr = 133.3224 Pa). In our experiments, pressure in the measurement cavity was monitored with an external pressure sensor (General Electric Druck DPI 142) as well as with the internal sensor. To shield the external sensor from humidity changes, it was installed in a dead end branched from the main line behind a drying cartridge filled with magnesium perchlorate. The pressure measurement line was branched directly upstream of the Picarro GHG analyzer (downstream for Flight-ready analyzers). To match the pressure inside the cavity to within a few Torr, a needle valve was installed as a choke upstream of the pressure measurement branch (downstream for Flight-ready analyzers). This setup allowed us to monitor pressure independently of water vapor content, while the internal pressure sensor still reacted to changes in water vapor levels in the sampling air.

The external pressure readings drifted on a timescale relevant for the gas washing bottle experiments. Therefore, in these experiments, dry air was measured between different water vapor levels to calibrate the external pressure readings. Each water vapor level (including dry air) was probed between 15 and 150 minutes (median about 40 minutes) depending on the stability of the external pressure measurement and trace gas readings. For further analysis, average readings from the Picarro



GHG analyzer and the external pressure sensor of the last 10 minutes of each probing interval were used. Some measurements with low water vapor levels with probing times of only about five minutes from an early experiment (Picarro GHG analyzer #1, see Table 1) were included as well. The order of water vapor levels was altered between experiments, including varying from wet to dry, dry to wet, and random switches between dryer and wetter air.

- 5 Experiments were performed with five Picarro GHG analyzers (Table 1).

2.2 Traditional parabolic water correction function

The effect of water on trace gas measurements made using Picarro GHG analyzers can be described by a water correction function $f_c(h)$, where c denotes the target gas (here: CO₂ or CH₄) and h is the water vapor mole fraction (measured by the Picarro analyzer). The analyzer measures the wet air mole fraction $c_{wet}(h)$, which is related to the dry air mole fraction c_{dry}
10 by the water correction function:

$$c_{dry} = \frac{c_{wet}(h)}{f_c(h)} \quad (1)$$

The traditional form of the water correction function takes into account dilution and line shape effects (details in Sect. 1). These are described by a second-degree Taylor series, i.e. a parabola:

$$f_c(h) = 1 + a_c \cdot h + b_c \cdot h^2 \quad (2)$$

The coefficients a_c and b_c can be derived from water correction experiments such as those described in Sect. 2.1.

3 Results

15 3.1 Links among external pressure measurement, CO₂, CH₄, H₂O and cavity pressure

To establish the link among the external pressure measurement, CO₂, CH₄, and internal cavity pressure for each Picarro GHG analyzer, the cavity pressure was varied manually using Picarro Inc. software in the range observed when varying water vapor content. Externally measured pressure, CO₂, and CH₄ varied linearly with internally monitored cavity pressure, with similar slopes for all instruments. As an example, the values for Picarro #3 obtained in dry air are shown in Table 2.
20 The water vapor measurement was not sensitive to cavity pressure. The slopes in wet air (3 % H₂O) were measured for Picarro #3 and were very similar to the slopes in dry air (CO₂: +5 %, CH₄: -2 %, cavity pressure: +1 %). Hence, internal cavity pressure, CO₂ and CH₄ were modeled as linear functions of externally measured pressure for subsequent analyses.

3.2 Dependency of cavity pressure on water vapor content

We monitored cavity pressure using an external sensor during gas washing bottle experiments (Sect. 2.1) for three different
25 Picarro GHG analyzers (Table 1). The pressure readings of the internal pressure sensors were, as expected, stable at 140 Torr with standard deviations of 0.015 Torr or less. To calculate a “corrected cavity pressure” from the external pressure



measurement, pressure readings for dry air before and after each wet air measurement were interpolated to the times of the wet air measurements. The deviations between the wet air pressure values and the interpolated dry air pressure values were multiplied with the slope described in Sect. 3.1, and added to the dry air cavity pressure of 140 Torr. The corrected cavity pressure obtained in this way varied systematically with the water vapor mole fraction of the sample air (Fig. 2). The variations displayed a uniform pattern for all three instruments. The pressure dropped in the presence of water vapor, and the gradient of pressure with respect to water vapor was larger between 0 and about 0.2 % H₂O than for higher water vapor content, exhibiting a “bend” where the two regimes meet. The deviations were up to 0.5 Torr for 3 % H₂O.

We describe the relationship between cavity pressure and water vapor mole fraction with an empirical function:

$$p(h) = p_0 + s \cdot h + d_p \cdot \left(e^{\frac{h}{h_p}} - 1 \right) \quad (3)$$

10

In this equation, p is the cavity pressure as determined from the external pressure measurement, h is the water vapor mole fraction, h_p is the position of the pressure bend described above, d_p is a measure for the pressure gradient at $0 \% < h < h_p$, p_0 is the pressure in dry air (fixed at 140 Torr), and s is the slope for $h \gg h_p$. Note that this empirical fit function is valid only in the water vapor range covered by measurements (see Fig. 2). Data from droplet experiments suggest that the pressure variation does not continue linearly along the slopes derived here at higher water vapor levels, so an extrapolation is not recommended.

15

All free parameters of the pressure model (s , d_p and h_p) varied between instruments (Table 3). For the empirical water correction functions for CO₂ and CH₄, only the pressure bend position (h_p) is relevant, as will be shown later. The mean estimate of h_p from all three experiments was (mean and standard deviation):

20

$$h_p = (0.079 \pm 0.014) \% \text{ H}_2\text{O} \quad (4)$$

3.3 Correction of the pressure effect on CO₂ and CH₄

Reliable data for both pressure and the target gases CO₂ and CH₄ were obtained in one experiment (with Picarro #3), which is presented in this section. Based on the data, four models were tested as potential water correction functions for CO₂ and CH₄ to examine performance, robustness, transferability, and consistency of the results. Model (i) was the traditional parabolic function, Eq. (2). The other three models represent different strategies to correct for the pressure effect. Model (ii) consisted of first correcting the pressure effect on the wet air mole fractions by estimating the pressure bias from Eq. (3) and then correcting the trace gas bias using the sensitivity of CO₂ and CH₄ to pressure (Table 2); then the traditional parabolic water correction was applied to the corrected wet air mole fractions. For models (iii) and (iv), the traditional parabolic model was expanded to account for the pressure effect. Since the trace gas readings of the analyzer varied linearly with pressure

25



(Sect. 3.1), the pressure effect was described as in Eq. (2), i.e. as a linear and a non-linear term. Since a linear dependency is already accounted for in the traditional parabolic model, the non-linear part of Eq. (2) was added to Eq. (3) to obtain a new model for the water correction:

$$f_c^p(h) = \frac{1 + a_c \cdot h + b_c \cdot h^2}{f_c(h)} + d_c \cdot \left(e^{\frac{h}{h_p}} - 1 \right) \quad (5)$$

The parameter d_c describes the magnitude of the pressure change at low water vapor contents and sensitivity of the target gas to the pressure change. The parameter h_p is the pressure bend position from Eq. (3). In model (iii), the parameters a_c , b_c , d_c and h_p from Eq. (5) were fitted to the trace gas data. Model (iv) was the same as model (iii) except that the pressure bend position h_p was set to the value obtained from the pressure data. Since all free parameters in model (iii) were estimated from the available trace gas data, this model was the most consistent with the data. Therefore, in subsequent analyses, we assumed that the fit to model (iii) yielded the true water correction function. Hence, we used the differences between the results from this model and the others as estimates of their biases.

The experiment was performed with dry air mole fractions of 404.0 ppm CO₂ and 1842 ppb CH₄. Water-corrected CO₂ and CH₄ data from this experiment are shown in Fig. 3. For CH₄, the most striking visible feature was the wave-like structure in the dry air mole fractions when using model (i), the traditional parabolic water correction function. The maximum negative bias of this model was 0.85 ppb at 0.17 % H₂O (corresponding to 0.046 % of the dry air mole fraction), and the maximum positive bias was 0.37 ppb at 1.7 % H₂O. Hence, the peak-to-peak difference was 1.2 ppb. The standard deviation of the dry air mole fractions estimated with this model was 0.35 ppb. By contrast, no structure was visible in the dry air mole fractions calculated with any of the three formulations taking into account the pressure change. This is reflected in the lower standard deviations of the dry air mole fractions, which were 0.20 ppb for model (ii), 0.17 ppb for model (iii) and 0.18 ppb for model (iv). This demonstrates the improvement achieved by correcting for the effect of pressure bias on CH₄.

The result from model (ii) yielded slightly larger deviations from the mean than models (iii) and (iv) in the range 0.1–0.3 % H₂O. These deviations were compatible with a sensitivity of CH₄ to cavity pressure changes of 80 % of the value inferred in Sect. 3.1, since at this value the results from model (ii) resemble the results from model (iv). This discrepancy is discussed in Sect. 4.3.

The pressure bend position estimated from the CH₄ data was $h_p = (0.059 \pm 0.015) \% \text{ H}_2\text{O}$. This is smaller than the estimate based on pressure data of $h_p = (0.095 \pm 0.011) \% \text{ H}_2\text{O}$. Despite this discrepancy, the two models yielded very similar dry air mole fractions, with differences within 0.12 ppb and a peak-to-peak difference of 0.22 ppb between 0.05 and 0.39 % H₂O. This demonstrates the robustness of the method against uncertainties in h_p .

The wave-like structure seen in the CH₄ dry air mole fractions estimated using the traditional parabolic water correction function was absent in the CO₂ data for this instrument. The standard deviations of the dry air mole fractions were similar for all models (model (i): 0.017 ppm, model (ii): 0.021 ppm, models (iii) and (iv): 0.014 ppm).



Using model (ii) induced a bias similar to the one present in the results of model (i) for CH₄ but with opposite sign (Fig. 3). This hints at an overcompensation of the pressure effect on CO₂. Indeed, following the same argument as for CH₄, the results of model (iv) were reproduced when the sensitivity of CO₂ to cavity pressure changes was set to 35 % of the value presented in Table 2. Note that the wave-like structure in CO₂ was apparent for one other instrument (Picarro #5, see Sect. 3.4 and 5 3.5.1). This has not been presented in this section since no external pressure sensor data were obtained for this instrument.

3.4 Consistency across instruments

To investigate whether common coefficients applicable to all Picarro GHG analyzers can be given for the enhanced water correction function, we performed water correction experiments with several Picarro GHG analyzers. Although reliable pressure and trace gas data from a single experiment were obtained for only one instrument (presented in Sect. 3.3), trace gas 10 data from water correction experiments were obtained for two more analyzers. The pressure effect on the trace gas data from these instruments differed in magnitude. Out of the three instruments for which trace gas data were investigated (Picarrros #3, #4, and #5), two exhibited the pressure effect visibly for CH₄ (Fig. 3 and Fig. 5; the exception was Picarro #4, see Fig. 4). In contrast, the CO₂ measurements of two instruments (#3 and #4) seemed to be unaffected by pressure changes (Fig. 3 and Fig. 4; the exception was Picarro #5, see Fig. 5). The differences make clear that common coefficients applicable to all Picarro 15 GHG analyzers can not be given based on our data. This is further discussed in Sect. 4.3 and Sect. 4.4.

3.5 Application to ambient measurements

In this section, we demonstrate the impact that the pressure effect has on ambient GHG observations from a site in northeast Siberia. The site is located in the remote village of Ambarchik on the coast of the Arctic Ocean (69.62° N, 162.30° E), and has been operational since August 2014. Air inlets are at 27 m and 14 m above ground level, and probed in turns for intervals 20 of 15 and 5 minutes, respectively. The gases CO₂ and CH₄ are measured in the humid air stream with a Picarro G2301 analyzer (Picarro #5). The measurements are calibrated automatically by measuring gas tanks calibrated to the WMO scales X2007 (CO₂) and X2004A (CH₄) every 116 hours.

3.5.1 Deriving coefficients for the improved water correction function without pressure data

In this section, we derive coefficients for the improved water correction function, Eq. (5), for CO₂ and CH₄ for the Picarro 25 G2301 analyzer operated in Ambarchik. For this instrument, one water correction experiment with the gas washing bottle method (see Sect. 2.1) was performed, using dry air from a pressurized tank with mole fractions of 352.9 ppm CO₂ and 1797 ppb CH₄. Cavity pressure was not monitored during this experiment. We estimated the parameters a_c , b_c and d_c from the trace gas data (Table 4 and Table 5), but the number of data points was insufficient to also estimate the pressure bend position h_p . Therefore, we used the mean h_p from the three experiments with external pressure monitoring, Eq. (4), and 30 investigated the uncertainty associated with this procedure.



As a conservative estimate, we considered an interval of three standard deviations around the mean a plausible range for h_p , i.e. $h_p \in [0.036, 0.122] \% \text{H}_2\text{O}$. Varying h_p in small steps within this interval, we fitted the other parameters of Eq. (5) to the trace gas data. To assess the uncertainty associated to using the mean h_p , we assumed that one of the h_p yielded the true water correction function for this instrument, and determined whether using the mean h_p could induce a larger error than using the traditional parabolic correction. For this assessment, we compared not only the data points obtained during the experiment, but sampled the fitted functions at 999 evenly spaced points over the range of H_2O covered during the experiment. For CO_2 , the maximum deviation between the function using the mean h_p and any other h_p in the plausible range was 0.007 ppm, while the best result for the maximum deviation between the traditional parabolic correction and the improved functions with h_p in the plausible range was 0.017 ppm. For CH_4 , the deviations were 0.20 ppb and 0.35 ppb, respectively. Therefore, maximum bias due to the uncertainty of h_p was smaller than the minimum bias when using the traditional parabolic correction for both CO_2 and CH_4 .

For reference, we also investigated the values for h_p estimated from the trace gas data. Fitting Eq. (5) to CH_4 yielded $h_p = (0.086 \pm 0.053) \% \text{H}_2\text{O}$, close to the mean h_p from the three pressure experiments but with a large uncertainty. For CO_2 , the fit yielded $h_p = (0.34 \pm 0.19) \% \text{H}_2\text{O}$, outside of the range considered plausible for h_p and again with a very large uncertainty. It may be argued that the plausible range h_p should be extended to 0.34 % H_2O . Using this extended range, the argument for the benefit of the improved water correction over the traditional one despite the uncertainty of h_p was weaker, but still held. However, we argue that the estimate $h_p = 0.34 \% \text{H}_2\text{O}$ is probably far from the true pressure bend position for this instrument. First, the estimate was based on CO_2 data, which were less consistent with pressure data than CH_4 data for another instrument (Sect. 3.3). Second, it is far from the pressure bend positions of all three instruments for which pressure data were obtained (Sect. 3.2). Third, the estimate was based on very few data points and was not robust against jackknife resampling (not shown). For these reasons, we consider h_p from Eq. (4) to be a realistic estimate for this Picarro analyzer.

To assess the bias of the traditional parabolic fit function, we assumed that the fit with pressure correction term using the mean h_p was the true water correction function. Maximum absolute deviations between the two were 0.037 ppm CO_2 and 0.78 ppb CH_4 at $\text{H}_2\text{O} = 0.16 \%$, and peak-to-peak deviations were 0.052 ppm CO_2 and 1.11 ppb CH_4 between $\text{H}_2\text{O} = 0.18 \%$ and 1.8 %. These deviations corresponded to biases of 0.0104 % CO_2 and 0.0437 % CH_4 . As an example, for dry air mole fractions of 400 ppm CO_2 and 2000 ppb CH_4 , the maximum absolute bias of the traditional water correction function would be 0.042 ppm CO_2 and 0.87 ppb CH_4 .

In Sect. 3.3, we compared the sensitivities of CO_2 and CH_4 to cavity pressure inferred from controlled cavity pressure changes with those inferred from water vapor changes for Picarro #3. We made the same comparison for Picarro #5 under the assumptions that the cavity pressure dependency on water vapor and the sensitivities of the trace gases to controlled cavity pressure changes were the same as for Picarro #3. The data from the water correction experiment were compatible with a sensitivity of CO_2 to cavity pressure change of 60 % of the value from controlled cavity pressure changes, which was



higher than the 35 % for Picarro #3. The corresponding number for CH₄ was 70 %, which more closely matched the 80 % of Picarro #3.

3.5.2 Impact of the improved water correction

In this section, we describe the impact of the improved water correction on hourly averages of CO₂ and CH₄ data from
5 Ambarchik over the years 2015 and 2016.

Differences between the traditional and improved water correction had a seasonal cycle following the seasonal cycle of water
vapor content in the sample air (Fig. 6). Maximum water vapor mole fractions occurred in July and August, when they
averaged around (0.9 ± 0.2) %. This was close to the water vapor content where the bias of the traditional parabolic water
corrections changed sign (Fig. 5). Hence, the summer biases averaged (0.00 ± 0.01) ppm CO₂ and (0.0 ± 0.2) ppb CH₄,
10 and were thus negligible. In winter, the water vapor content was in the range of the pressure bend position, where the bias
was highest. The maximum monthly biases occurred in April and were -0.037 ppm CO₂ and -0.75 ppb CH₄. From December
to March, water vapor content episodically dropped well below the pressure bend position (this occurred when the air
temperature dropped below about -25°C), thus the bias decreased. During the coldest temperatures, which occurred in
February, the biases were -0.02 ppm CO₂ and -0.5 ppb CH₄.

15 We also investigated the effect of the improved water correction on dry air calibrations at this site (data not shown).
Calibrations were performed with calibrated dry air gas tanks periodically. The measurement system was flushed with dry air
for at least 13 minutes before data were used. This left so little water vapor in the system that the remaining effects were
negligible.

3.6 Evaluation of droplet experiments for the improved water correction

20 Droplet experiments are a quick and simple method to obtain data for correcting the influence of water vapor on a Picarro
GHG analyzer (Rella et al., 2013). We performed a series of droplet experiments (details on the setup are given in Sect. 2.1)
with Picarro #1, and derived coefficients for the improved water correction function, Eq. (5), for CO₂ and CH₄. We used data
below 3.5 % H₂O and where the difference between subsequent H₂O measurements was less than 0.005 %. The latter was an
empirical filter to exclude the fastest water vapor variations while leaving enough data for fitting. The temporal variation of
25 water vapor during these experiments was fastest during evaporation of the last bits of the droplets, i.e. during the transition
from about 0.5–1 % to 0 % H₂O (Fig. 7). As determined in the gas washing bottle experiments, this was the domain of
fastest pressure variations, and the pressure during these experiments was consistently too low in this domain, with large
variations between the experiments (Fig. 8). We discuss this deviation in Sect. 4.5.

Consequently, differences between water correction fits were expected. Indeed, the differences between the fit functions for
30 the different droplets were extremely large around the pressure bend position (0.17 ppm CO₂ between droplets 2 and 4 at
0.29 % H₂O and 6.0 ppb CH₄ between droplets 1 and 2 at 0.18 % H₂O; Fig. 9). When fixing the pressure bend position to the
value from the gas washing bottle experiment for this instrument ($h_p = 0.066$ % H₂O), the scatter increased to 0.24 ppm



CO₂ and 6.4 ppb CH₄. The scatter reduced to 0.04 ppm CO₂ and 1.2 ppb CH₄ when applying the traditional parabolic fit to these data, which illustrates that the experiments were consistent apart from the final drop of the water vapor mole fraction to 0 % H₂O, where the pressure changed most rapidly.

4 Discussion

5 4.1 Dependency of cavity pressure on water vapor content

Our results demonstrate that the cavity pressure of Picarro GHG analyzers is sensitive to the water vapor content of the measured air. This effect influences the dependency of CO₂ and CH₄ on water vapor.

4.1.1 Possible underlying effect

We speculate that the observed sensitivity of internal pressure readings to humidity levels in the sampling air is due to adsorption of H₂O molecules on the pressure sensor inside the cavity. This sensor controls the outlet valve of the cavity (inlet valve for Flight-ready analyzers) to keep the cavity pressure stable. The pressure measurement is based on a piezoresistive strain gauge exposed to the pressure media (air in the cavity). The strain gauge is mounted on a thin diaphragm, which is deflected by air pressure. The resulting strain causes a change in electrical resistance and creates an output voltage varying with pressure. Water molecules adsorbed on the strain gauge, diaphragm, or adjacent parts of the sensor may change its response to pressure mechanically, and/or may affect the electrical properties of the circuit. If either or both were the case, the deviating pressure readings during droplet experiments could be due to an equilibration time of the adsorption process. Indeed, the largest pressure deviations were observed when the water content changed fastest (Fig. 7 and Fig. 8). However, elucidating the underlying physical effect of the pressure changes is beyond the scope of this paper, and was not investigated further.

20 4.1.2 Uncertainties of the external pressure measurement

The sensitivities of the external pressure measurement to cavity pressure were derived by manually varying cavity pressure (Sect. 3.1). It is possible that the relationships do not hold for variations of water vapor. One potential influence is the drying agent in the line of the external pressure sensor, which may affect the sensor readings due to the differences in partial pressure of water vapor. Additionally, the flow through the needle valves used as chokes to match the external pressure to cavity pressure may be sensitive to water vapor.

To investigate these possible effects, we measured the sensitivity of the external pressure measurement to cavity pressure in dry and wet air (3 % H₂O) for Picarro #3, and found no difference (Sect. 3.1). This indicates that cavity pressure is indeed well-represented by the external pressure measurement in equilibrium.

Note that, for the empirical correction of the pressure effect on CO₂ and CH₄, pressure data were used only if the data obtained in a water correction experiment were insufficient to constrain all parameters of the improved water correction



function (Sect. 3.5.1). As long as sufficient data are available, uncertainties in our pressure data are of no importance for the empirical water correction.

4.2 Improvement over traditional parabolic water correction function

As described in Sect. 3.1, CO₂ and CH₄ depend linearly on pressure. Consequently, the pressure bend (Fig. 2) is featured in the trace gas data as well. This behavior cannot be modeled with the traditional parabolic water correction function, and hence causes biases in dry air mole fractions derived with the traditional correction. For some instruments, the pressure bend was visible as water-dependent bias when using parabolas as water correction functions (Fig. 3 and Fig. 5). The improved water correction function, Eq. (5), resulted in residuals without systematic structure. The bias observed between the traditional and improved water correction functions was up to 0.037 ppm CO₂ (Picarro #5, dry air mole fraction 352.9 ppm) and 0.85 ppb CH₄ (Picarro #3, dry air mole fraction 1842 ppb), with peak-to-peak differences of up to 0.052 ppm CO₂ and 1.2 ppb CH₄, which can appear in ambient air measurements as seasonal cycles or as differences between sites depending on humidity differences.

To derive water correction coefficients for an instrument, enough data must be available to constrain at least the sensitivity of CO₂ and CH₄ to the pressure effect. If not enough data are available to constrain the pressure bend position, it may be possible to use the mean value from our experiments, $h_p = (0.079 \pm 0.014) \% \text{ H}_2\text{O}$. If this is attempted, one must investigate whether the uncertainty in the pressure bend position may introduce a larger bias than the traditional water correction function (Sect. 3.5.1).

4.3 Inconsistencies between trace gas- and pressure data

In Sect. 3.3, we found that correcting for the pressure effect on CO₂ and CH₄ by using the pressure bias and the sensitivities of the trace gas measurements to cavity pressure during controlled pressure changes (model (ii)) overcompensates the pressure effect. There are two possible explanations: (1) the external pressure measurement may have overestimated the changes in cavity pressure, or (2) the trace gas mole fractions delivered to the analyzer varied systematically with water vapor. If explanation (1) were true, the sensitivity of the external pressure sensor reading to controlled cavity pressure changes (Sect. 3.1) would have been different than to changes due to water vapor. There is no evidence for such an effect (Sect. 4.1.2). Furthermore, CO₂ and CH₄ would have been affected in the same way, which was not the case, which makes this hypothesis unlikely. Explanation (2) seems more likely, since overall CO₂ results were less robust than those for CH₄. We observed no visible pressure effect at all on CO₂ from two out of three instruments (Fig. 3 and Fig. 4). In one of these instruments (#3), the pressure effect was seen in CH₄ in the same experiment (Fig. 3). The fact that CO₂ and CH₄ behaved differently suggests that the inconsistent results for CO₂ were due to the variations in the mole fraction delivered to the Picarro analyzer. A difference between the two gases is the higher solubility of CO₂ in water, which makes it difficult to deliver a constant CO₂ mole fraction to the analyzer under varying humidity. However, we carefully observed the equilibration of trace gas mole fractions during the experiments. It is possible that an equilibration effect was at play at a



time scale much longer than an hour, since this may have gone unobserved in our experiments. If this explanation were true, the systematic difference between dry air and wet air trace gas mole fractions would have precisely compensated for the pressure bend, which seems unlikely.

Thus, the reason for the poor performance of model (ii) in Sect. 3.3, and the apparent absence of the effect especially on CO₂ in some cases remains unclear. We recommend not using model (ii), and instead deriving all coefficients from the trace gas data. This implies that, to correct for the pressure effect, no external pressure measurement is necessary. We also recommend considering using the pressure bend position derived from CH₄ data for CO₂ in case of discrepancies, because the CH₄ data appeared more consistent with the pressure data in our experiments.

4.4 Transferability of the correction function to other instruments

The form of the pressure dependency on water vapor was the same for all instruments tested. The magnitude of the effect on CO₂ and CH₄ differed across instruments. In some cases, the effect on CO₂ (two out of three instruments) and CH₄ (one of these two instruments) even appeared negligible. In those cases, it may be possible that a small effect exists but is masked by random fluctuations. Therefore, correction coefficients for the water correction have to be obtained for each Picarro GHG analyzer individually.

4.5 Effect on dry air calibrations

The fact that the pressure effect is largest in almost dry air and our experience with equilibration effects during droplet experiments led us to investigate whether the pressure effect is relevant for calibration measurements with dry air. At the Ambarchik site, very little water vapor was left during dry air calibrations, and the improved water correction had a negligible effect on the calibrations. However, the improvement may be relevant when residual water levels are higher. When switching from humid ambient air to a dry air gas tank, cavity pressure changes quickly. Hence, pressure equilibration may influence the trace gas data despite low residual water levels similarly as we observed during droplet experiments. This highlights the need to allow time for pressure equilibration during calibration measurements using dry air (see Sect. 4.6 about the calibration time).

4.6 Droplet experiments

We attempted to correct the pressure effect using data from droplet experiments and found inconsistent results (Sect. 3.6). The key difference between droplet experiments and gas washing bottle experiments is the temporal variation of water vapor in the air stream. During gas washing bottle experiments, the median probing time of a water vapor level was 40 minutes. After this time, the pressure- and trace gas readings all appeared to be in equilibrium. This included the external pressure reading, which may have had longer equilibration times than cavity pressure. The temporal variation of water vapor content during droplet experiments was somewhat random, but in general, the droplets dried up very quickly after sustaining a level of about 0.5 to 1 % H₂O for several minutes. Since this behavior matched our previous experiences with the droplet method



(not shown), we generalize the implications. The fast drop to 0 % H₂O has two implications for the correction of the pressure bend: (i) few data are available for fitting, and (ii) there is not enough time for the internal pressure sensor to equilibrate, which means it will always be influenced by the water vapor content during at least the last few minutes. Since the water vapor content generally decreases over time in droplet experiments, the pressure readings during fast water vapor variations will in most cases be too low, especially during the fast drop to 0 % H₂O. This pattern is demonstrated in Fig. 8, which also shows that cavity pressure was closest to equilibrium during the droplet experiment with the slowest H₂O variation before the droplet dried up. Since we have no reliable CO₂ and CH₄ data from a gas washing bottle experiment for this instrument, we could not make a direct comparison of the water correction functions obtained using droplets and using the gas washing bottle method. However, since the pressure deviation was systematic, we argue that the pressure effect is in general exaggerated by droplet data. The large scatter between the water correction functions based on the different droplets is illustrated in Fig. 9, highlighting that this method does not provide stable-enough signals to derive coefficients for the improved water correction function.

4.7 Impact of the improved water correction function on inversions of atmospheric transport

We observed biases persistent over several weeks of around 40 % of the WMO goals (80 % for CO₂ in the southern hemisphere) in field data when we applied the traditional parabolic water correction (Sect. 4.2).

Several studies have assessed the impact of observation bias on retrieved fluxes for CO₂ (Masarie et al., 2011; Peters et al., 2010; Rödenbeck et al., 2006). The results indicated small impacts of observation biases considerably larger than the WMO goals on annual flux budgets at continental scales. The flux results were more sensitive to model errors such as imperfect atmospheric transport and coarse resolution of the transport and flux model, and differences in the prior flux fields. This suggests that the biases of the traditional water correction function probably only have a small impact on retrieved fluxes. However, the observation bias scenarios in these studies were different than the patterns expected from the traditional water correction. For instance, a bias with a seasonal cycle has not been investigated. In most scenarios, only few stations out of the whole station network used for optimizing fluxes were assigned a bias (Masarie et al., 2011; Rödenbeck et al., 2006), whereas Picarro GHG analyzers are widely used, so that larger parts of station networks can be affected. Furthermore, there may be larger impacts at smaller spatial scales. Despite the small impact of measurement biases on the order of the WMO goals in current inversion systems, the pursuit of measurement uncertainties within the WMO goals is important for several reasons such as future model developments, which may decrease model errors and thus increase the relevance of observation biases (Masarie et al., 2011).

We are not aware of similar bias impact studies for methane. Given the similarity of the corrected biases of CO₂ and CH₄ with respect to the WMO goals, we expect similarly small impacts for CH₄ as for CO₂.



5 Conclusions

We reported previously undocumented biases of CO₂ and CH₄ measurements obtained with Picarro GHG analyzers in humid air. The biases are due to a sensitivity of the pressure in the measurement cavity to water vapor. We speculate that the underlying physical mechanism is adsorption of water molecules on the piezoresistive pressure sensor in the cavity that is used to keep the pressure constant. The pressure changes affect the water dependency of the CO₂ and CH₄ measurements. The most important feature of the effect is a transition of the rate of cavity pressure change with respect to water vapor below 0.2 % H₂O. This pressure bend propagates into the CO₂ and CH₄ measurements and is not modeled well by the traditional parabolic water correction function commonly used for Picarro GHG analyzers, causing water-dependent bias.

To correct for the pressure effect, we proposed an empirical expansion of the traditional water correction. The improved function eliminated the visible systematic offsets in the dry air mole fractions of CO₂ and CH₄ in our water correction experiments. We observed the bias caused by using the traditional parabolic water correction function to be largest in the range 0.05 % < H₂O < 0.5 %. The largest biases were 0.037 ppm CO₂ (corresponding to 0.010 % of the dry air mole fraction) and 0.85 ppb CH₄ (0.046 % of the dry air mole fraction), which are 40 % of the WMO inter-laboratory compatibility goals (80 % for CO₂ in the southern hemisphere). Maximum relative biases between dry air mole fractions derived using the traditional model were 0.052 ppm CO₂ and 1.2 ppb CH₄.

Our experimental results were more robust for CH₄ than for CO₂ in that the CH₄ data were more consistent with the pressure data. Although the reason behind this is not entirely clear, we speculate that it was due to experimental limitations caused by the higher solubility of CO₂ in water.

The magnitude of the effect differed between instruments and ranged from being negligible to the values reported above.

Possible changes in the pressure effect over time were not investigated.

Although the functional form was consistent across instruments, coefficients have to be determined for each analyzer individually, since we found differences in the magnitude of the effect. It may be possible to use the average pressure bend position found in our experiments for the correction function of other Picarro GHG analyzers, should existing water correction data not suffice to constrain it. We introduced a method to investigate whether this approach may introduce an error larger than the bias of the traditional water correction function.

To obtain coefficients for the improved water correction function, no pressure data are necessary. Instead, coefficients should be determined directly from CO₂ and CH₄ data from a water correction experiment. We recommend considering using the pressure bend position derived from CH₄ data for CO₂ in case of discrepancies, because the CH₄ data appeared more consistent with the pressure data in our experiments. Water correction experiments must be designed in a way that allows holding the water vapor mole fraction constant at a defined level to obtain a data point, thus allowing pressure equilibration. During the commonly used droplet experiments, water vapor content in the sample air typically varies quickly around the pressure bend position. This causes a systematic overestimation with large uncertainties of the pressure effect. Therefore, the droplet method is not suitable for obtaining coefficients for the improved water correction function. This



observation further implies that calibrations of Picarro GHG analyzers using dry air must be long enough to allow pressure equilibration (see Sect. 4.6 about the calibration time).

Our work revealed water-dependent biases in the measurements of dry air mole fractions of CO₂ and CH₄ in humid air obtained using the traditional parabolic water correction function for Picarro GHG analyzers. The biases can reach
5 considerable portions of the WMO inter-laboratory compatibility goals. We provided a way for eliminating the biases with an improved water correction function.

6 Acknowledgements

This work was supported by the Max-Planck Society, the European Commission (PAGE21 project, FP7-ENV-2011, grant agreement No. 282700, and PerCCOM project, FP7-PEOPLE-2012-CIG, grant agreement No. PCIG12-GA-201-333796),
10 the German Ministry of Education and Research (CarboPerm-Project, BMBF grant No. 03G0836G), the AXA Research Fund (PDOC_2012_W2 campaign, ARF fellowship M. Göckede), and the European Science Foundation (TTorch Research Networking Programme, Short Visit Grant F. Reum). We thank Stephan Baum, Dietrich Feist and Steffen Knabe (MPI-BGC) for help with the experiments. We thank David Hutcherson (Amphenol Thermometrics (UK) Ltd) for clarifications regarding the piezoresistive pressure measurement technique and Andrew Durso (MPI-BGC) for proofreading the
15 manuscript.

7 References

- Chen, H., Winderlich, J., Gerbig, C., Hofer, A., Rella, C. W., Crosson, E. R., Van Pelt, A. D., Steinbach, J., Kolle, O., Beck, V., Daube, B. C., Gottlieb, E. W., Chow, V. Y., Santoni, G. W. and Wofsy, S. C.: High-accuracy continuous airborne measurements of greenhouse gases (CO₂ and CH₄) using the cavity ring-down spectroscopy (CRDS) technique, Atmos.
20 Meas. Tech., 3(2), 375–386, doi:10.5194/amt-3-375-2010, 2010.
- Crosson, E. R.: A cavity ring-down analyzer for measuring atmospheric levels of methane, carbon dioxide, and water vapor, Appl. Phys. B Lasers Opt., 92, 403–408, doi:10.1007/s00340-008-3135-y, 2008.
- Kirschke, S., Bousquet, P., Ciais, P., Saunoy, M., Canadell, J. G., Dlugokencky, E. J., Bergamaschi, P., Bergmann, D., Blake, D. R., Bruhwiler, L., Cameron-Smith, P., Castaldi, S., Chevallier, F., Feng, L., Fraser, A., Heimann, M., Hodson, E.
25 L., Houweling, S., Josse, B., Fraser, P. J., Krummel, P. B., Lamarque, J.-F., Langenfelds, R. L., Le Quére, C., Naik, V., O’Doherty, S., Palmer, P. I., Pison, I., Plummer, D., Poulter, B., Prinn, R. G., Rigby, M., Ringeval, B., Santini, M., Schmidt, M., Shindell, D. T., Simpson, I. J., Spahni, R., Steele, L. P., Strode, S. A., Sudo, K., Szopa, S., van der Werf, G. R., Voulgarakis, A., van Weele, M., Weiss, R. F., Williams, J. E. and Zeng, G.: Three decades of global methane sources and sinks, Nat. Geosci., 6(10), 813–823, doi:10.1038/ngeo1955, 2013.
- 30 Masarie, K. A., Pétron, G., Andrews, A., Bruhwiler, L., Conway, T. J., Jacobson, A. R., Miller, J. B., Tans, P. P., Worthy, D.



- E. and Peters, W.: Impact of CO₂ measurement bias on CarbonTracker surface flux estimates, *J. Geophys. Res. Atmos.*, 116(17), 1–13, doi:10.1029/2011JD016270, 2011.
- McGuire, A. D., Christensen, T. R., Hayes, D., Herault, A., Euskirchen, E., Kimball, J. S., Koven, C., Lafleur, P., Miller, P. A., Oechel, W. C., Peylin, P., Williams, M. and Yi, Y.: An assessment of the carbon balance of Arctic tundra: comparisons among observations, process models, and atmospheric inversions, *Biogeosciences*, 9(8), 3185–3204, doi:10.5194/bg-9-3185-2012, 2012.
- Nara, H., Tanimoto, H., Tohjima, Y., Mukai, H., Nojiri, Y., Katsumata, K. and Rella, C. W.: Effect of air composition (N₂, O₂, Ar, and H₂O) on CO₂ and CH₄ measurement by wavelength-scanned cavity ring-down spectroscopy: Calibration and measurement strategy, *Atmos. Meas. Tech.*, 5(11), 2689–2701, doi:10.5194/amt-5-2689-2012, 2012.
- 10 Peters, W., Krol, M. C., van der Werf, G. R., Houweling, S., Jones, C. D., Hughes, J., Schaefer, K., Masarie, K. A., Jacobson, A. R., Miller, J. B., Cho, C. H., Ramonet, M., Schmidt, M., Ciattaglia, L., Apadula, F., Heltai, D., Meinhardt, F., di Sarra, A. G., Piacentino, S., Sferlazzo, D., Aalto, T., Hatakka, J., Ström, J., Haszpra, L., Meijer, H. A. J., van Der Laan, S., Neubert, R. E. M., Jordan, A., Rodó, X., Morguí, J. A., Vermeulen, A. T., Popa, E., Rozanski, K., Zimnoch, M., Manning, A. C., Leuenberger, M., Uglietti, C., Dolman, A. J., Ciais, P., Heimann, M. and Tans, P.: Seven years of recent European net
- 15 terrestrial carbon dioxide exchange constrained by atmospheric observations, *Glob. Chang. Biol.*, 16(4), 1317–1337, doi:10.1111/j.1365-2486.2009.02078.x, 2010.
- Rella, C. W., Chen, H., Andrews, A. E., Filges, A., Gerbig, C., Hatakka, J., Karion, A., Miles, N. L., Richardson, S. J., Steinbacher, M., Sweeney, C., Wastine, B. and Zellweger, C.: High accuracy measurements of dry mole fractions of carbon dioxide and methane in humid air, *Atmos. Meas. Tech.*, 6(3), 837–860, doi:10.5194/amt-6-837-2013, 2013.
- 20 Rödenbeck, C., Conway, T. J. and Langenfelds, R. L.: The effect of systematic measurement errors on atmospheric CO₂ inversions: a quantitative assessment, *Atmos. Chem. Phys.*, 6(6), 149–161, doi:10.5194/acp-6-149-2006, 2006.
- Winderlich, J., Chen, H., Gerbig, C., Seifert, T., Kolle, O., Lavrič, J. V., Kaiser, C., Höfer, A. and Heimann, M.: Continuous low-maintenance CO₂/CH₄/H₂O measurements at the Zotino Tall Tower Observatory (ZOTTO) in Central Siberia, *Atmos. Meas. Tech.*, 3(4), 1113–1128, doi:10.5194/amt-3-1113-2010, 2010.
- 25 WMO: 18th WMO/IAEA Meeting on Carbon Dioxide, Other Greenhouse Gases and Related Tracers Measurement Techniques (GGMT-2015). [online] Available from: https://library.wmo.int/opac/doc_num.php?explnum_id=3074, 2016.



Table 1: Overview of experiments.

Label	Name	Model	Type	Droplet experiment	Gas washing bottle experiment	External pressure measurement
#1	CFKBDS2004	G2401-m	Flight-ready	Yes	Yes	Yes
#2	CFKADS2199	G2401	Ground	No	Yes	Yes
#3	CFKBDS2108	G2401-m	Flight-ready	No	Yes	Yes
#4	CFKBDS2003	G2401-mc	Flight-ready	Yes	Yes	No
#5	CFADS2347	G2301	Ground	Yes	Yes	No

5

10

15

20

25



Table 2: Relationships between external pressure measurement, CO₂ and CH₄, and internal cavity pressure expressed as slopes (estimate and standard error) with respect to the external pressure measurement. Values shown here were derived for Picarro #3 with dry air and mole fractions of 404.0 ppm CO₂ and 1842 ppb CH₄.

Cavity pressure	$(1.04 \pm 0.0008) \text{ Torr Torr}^{-1}$
CO ₂	$(0.502 \pm 0.0006) \text{ ppm Torr}^{-1}$
CH ₄	$(8.25 \pm 0.006) \text{ ppb Torr}^{-1}$

5

10

15

20

25

30



Table 3: Fit coefficients (estimate and standard error) from Eq. (3) for three Picarro GHG analyzers

Picarro analyzer	s [Torr (% H ₂ O) ⁻¹]	h_p [% H ₂ O]	d_p [Torr]
#1	-0.17 ± 0.012	0.066 ± 0.0092	0.18 ± 0.012
#2	-0.14 ± 0.0042	0.076 ± 0.009	0.14 ± 0.0065
#3	-0.076 ± 0.0047	0.095 ± 0.011	0.21 ± 0.0092

5

10

15

20

25



Table 4: Water correction coefficients for Picarro #5 based on Eq. (5). The parameter h_p was taken from Eq. (4). See also Table 5.

Species	a_c [(% H ₂ O) ⁻¹]	b_c [(% H ₂ O) ⁻²]	d_c [unitless]
CO ₂	$(-1.539 \pm 0.005) \times 10^{-2}$	$(3.4 \pm 1.6) \times 10^{-5}$	$(1.6 \pm 0.3) \times 10^{-4}$
CH ₄	$(-1.30 \pm 0.02) \times 10^{-2}$	$(1.9 \pm 5.2) \times 10^{-5}$	$(6.6 \pm 1.0) \times 10^{-4}$

5

10

15

20

25

30



Table 5: Same as Table 4, but for fits using $\text{H}_2\text{O}_{\text{rep}}$ instead of H_2O for comparability of the coefficients a_c and b_c to previous studies (Chen et al., 2010; Rella et al., 2013). Dry air mole fractions obtained with either set of coefficients were virtually identical ($\Delta\text{CO}_2 < \pm 0.0008$ ppm and $\Delta\text{CH}_4 < \pm 0.002$ ppb; results for the coefficients reported in Table 4 are in Fig. 5), and for subsequent analyses the coefficients reported in Table 4 were used.

Species	$a_c [(\% \text{H}_2\text{O}_{\text{rep}})^{-1}]$	$b_c [(\% \text{H}_2\text{O}_{\text{rep}})^{-2}]$	d_c [unitless]
CO_2	$(-1.189 \pm 0.004) \times 10^{-2}$	$(-2.7 \pm 0.1) \times 10^{-4}$	$(1.5 \pm 0.3) \times 10^{-4}$
CH_4	$(-1.01 \pm 0.01) \times 10^{-2}$	$(-2.4 \pm 0.4) \times 10^{-4}$	$(6.6 \pm 1.1) \times 10^{-4}$

5

10

15

20

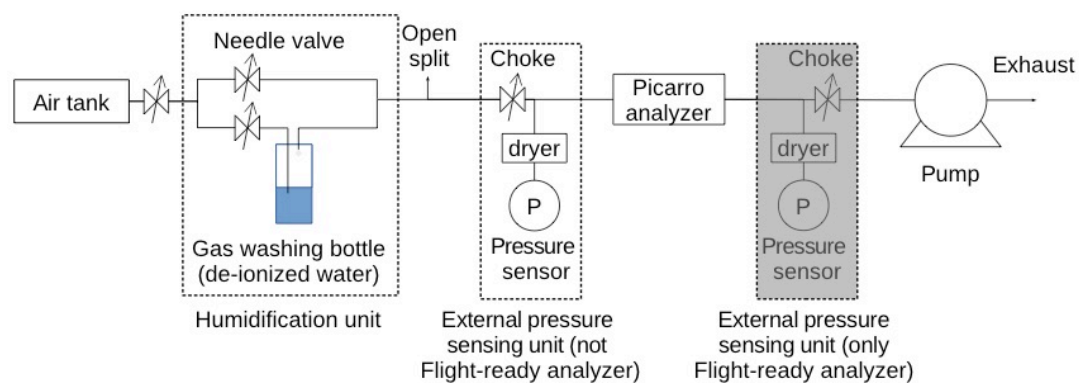


Fig. 1: Experimental setup used for the water correction experiments. For Flight-ready analyzers, the external pressure sensor was installed downstream of the analyzer, instead of upstream. For droplet experiments, the humidification unit was replaced by a tee piece.

5

10

15

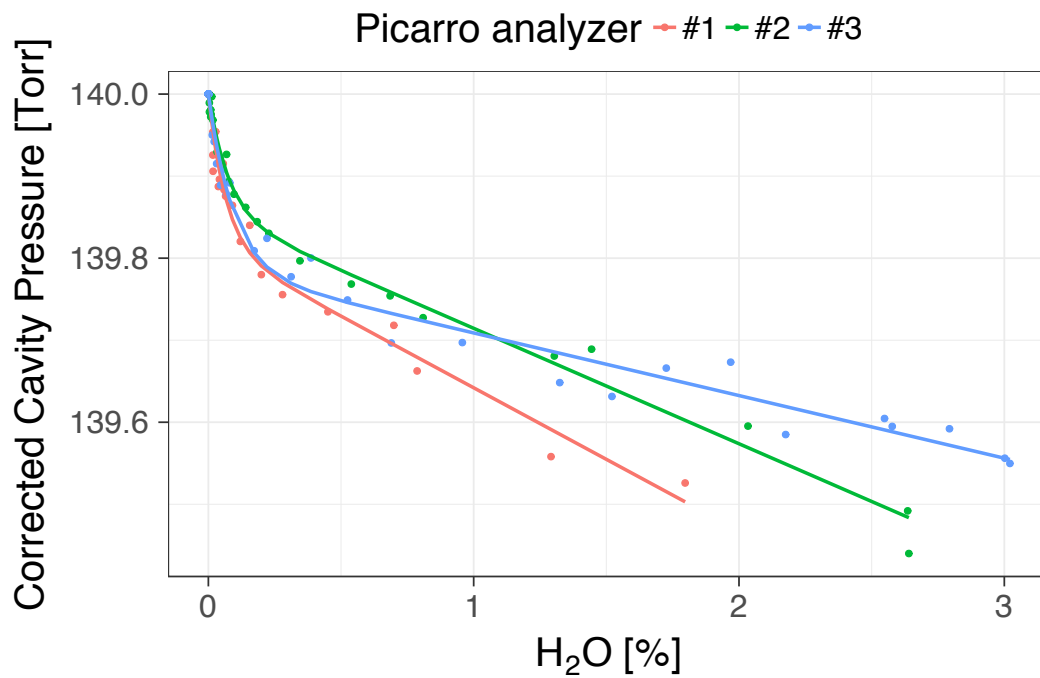


Fig. 2: Cavity pressure as a function of water vapor for three Picarro GHG analyzers. The lines are the fits to Eq. (3).

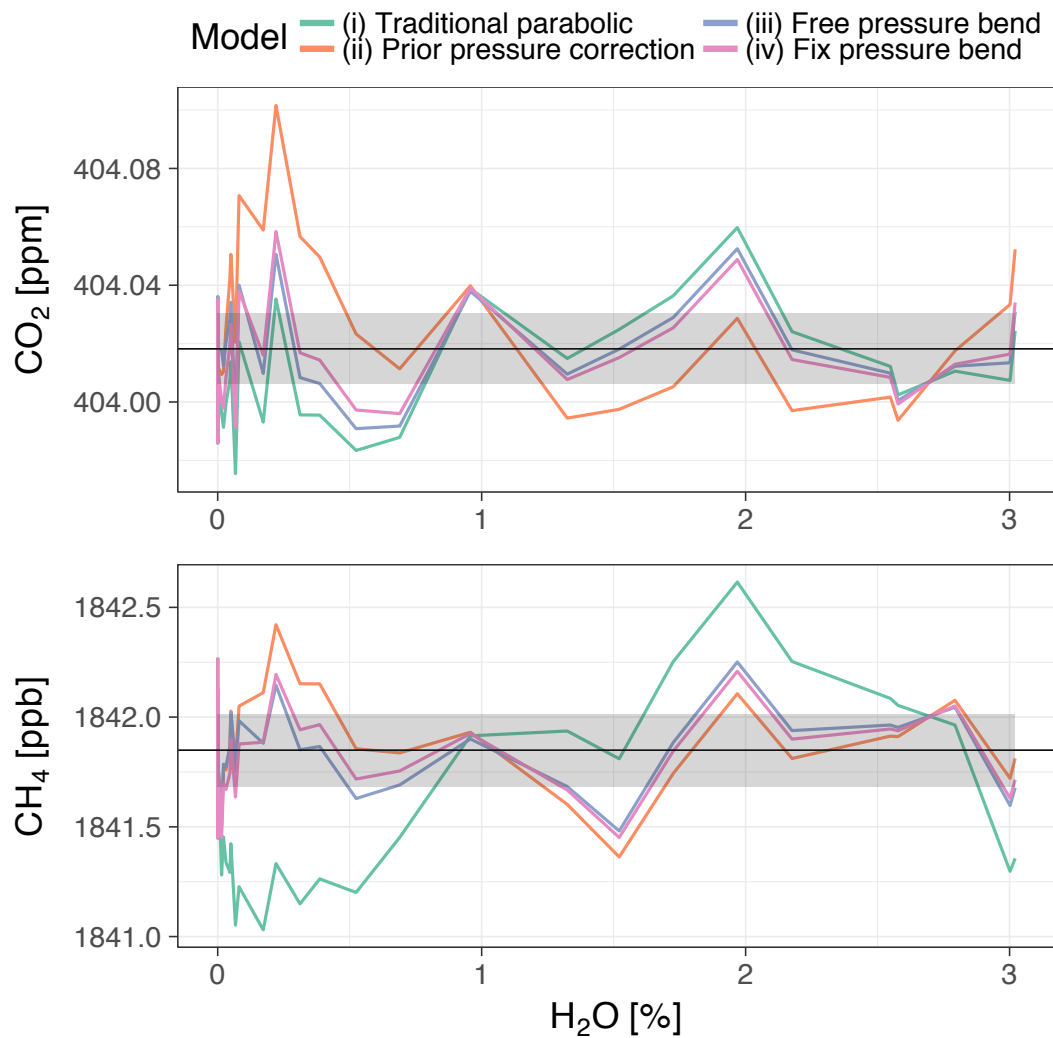


Fig. 3: CO₂ and CH₄ dry air mole fractions for Picarro #3 based on the four water correction functions described in the text. The grey bar denotes one standard deviation of the trace gas during the dry air measurements that were obtained between different water vapor levels.

5

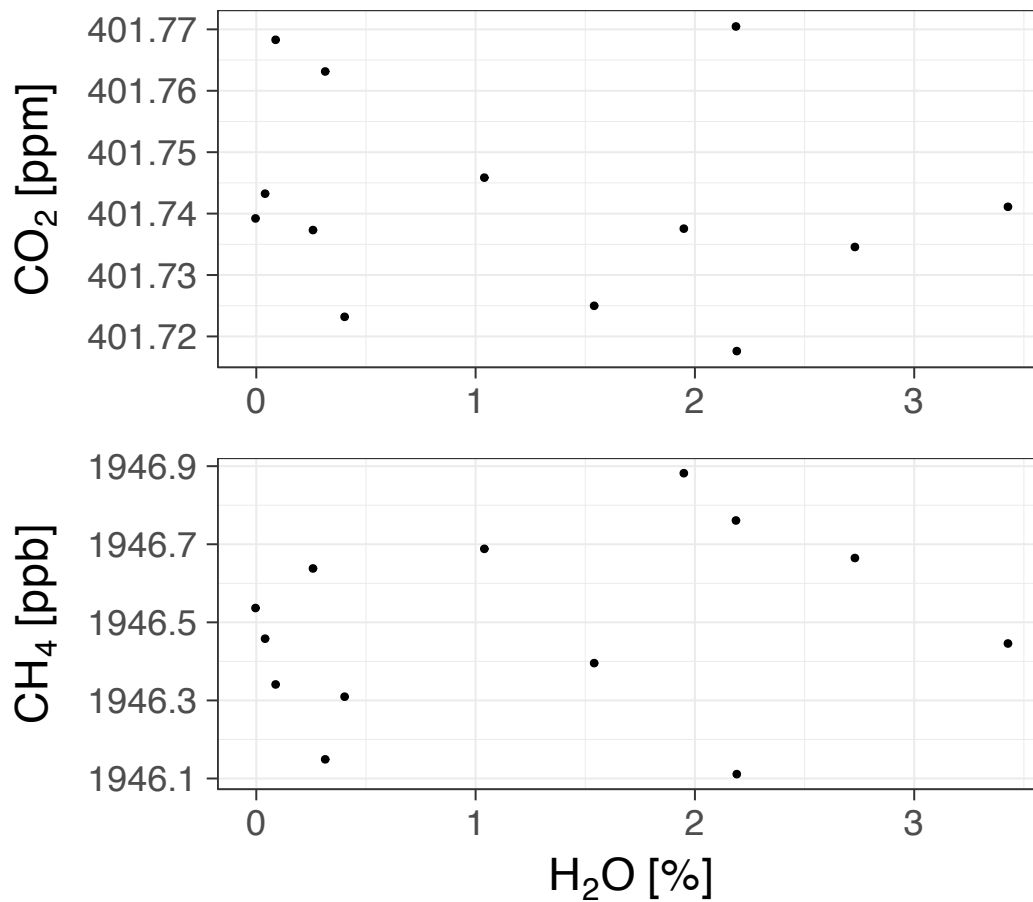


Fig. 4: Dry air mole fractions of CO₂ and CH₄ for a gas washing bottle experiment with Picarro #4 based on the traditional parabolic water correction function. No systematic biases are obvious.

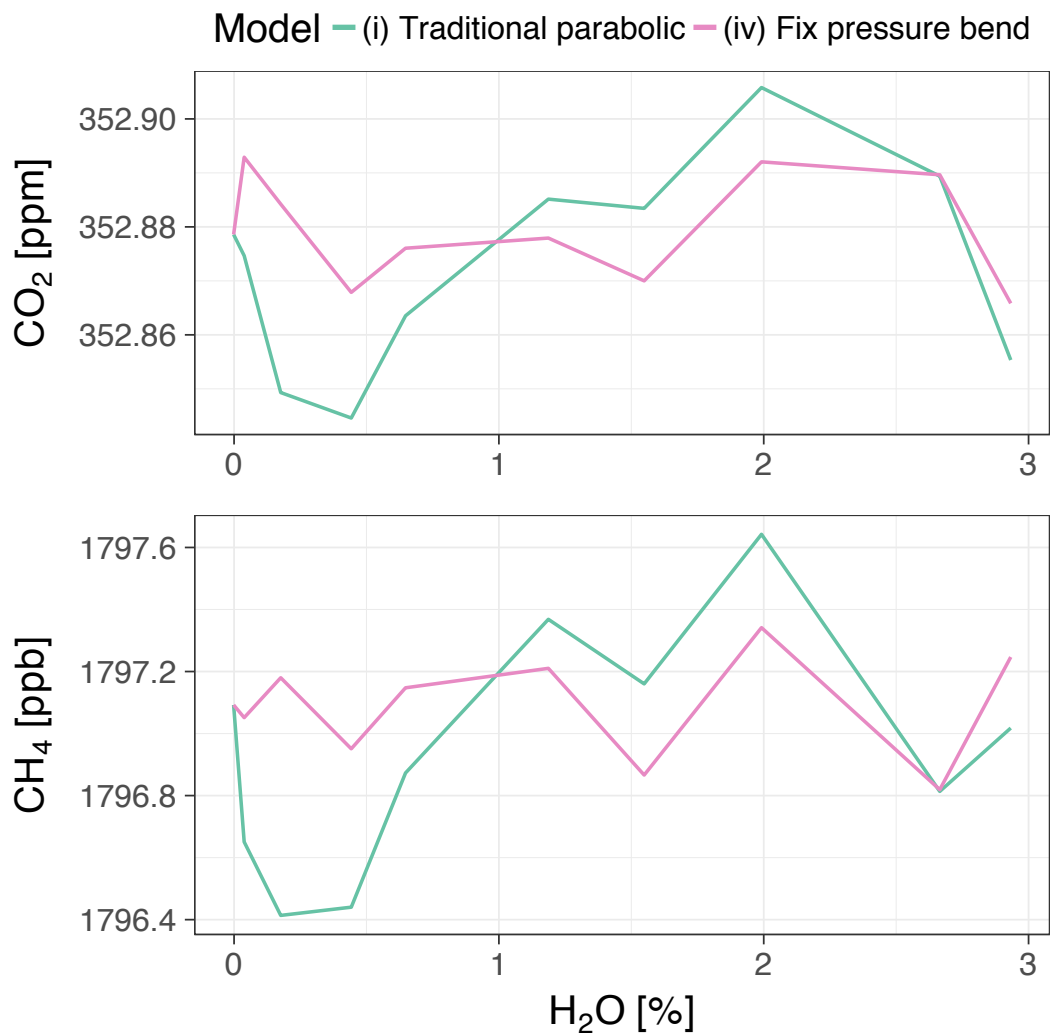


Fig. 5: Dry air mole fractions of CO₂ and CH₄ for Picarro #5 from a gas washing bottle experiment. Shown here are results for the traditional parabolic water correction function, and the improved water correction function using h_p from Eq. (4) (model (iv); see also Sect. 3.3).

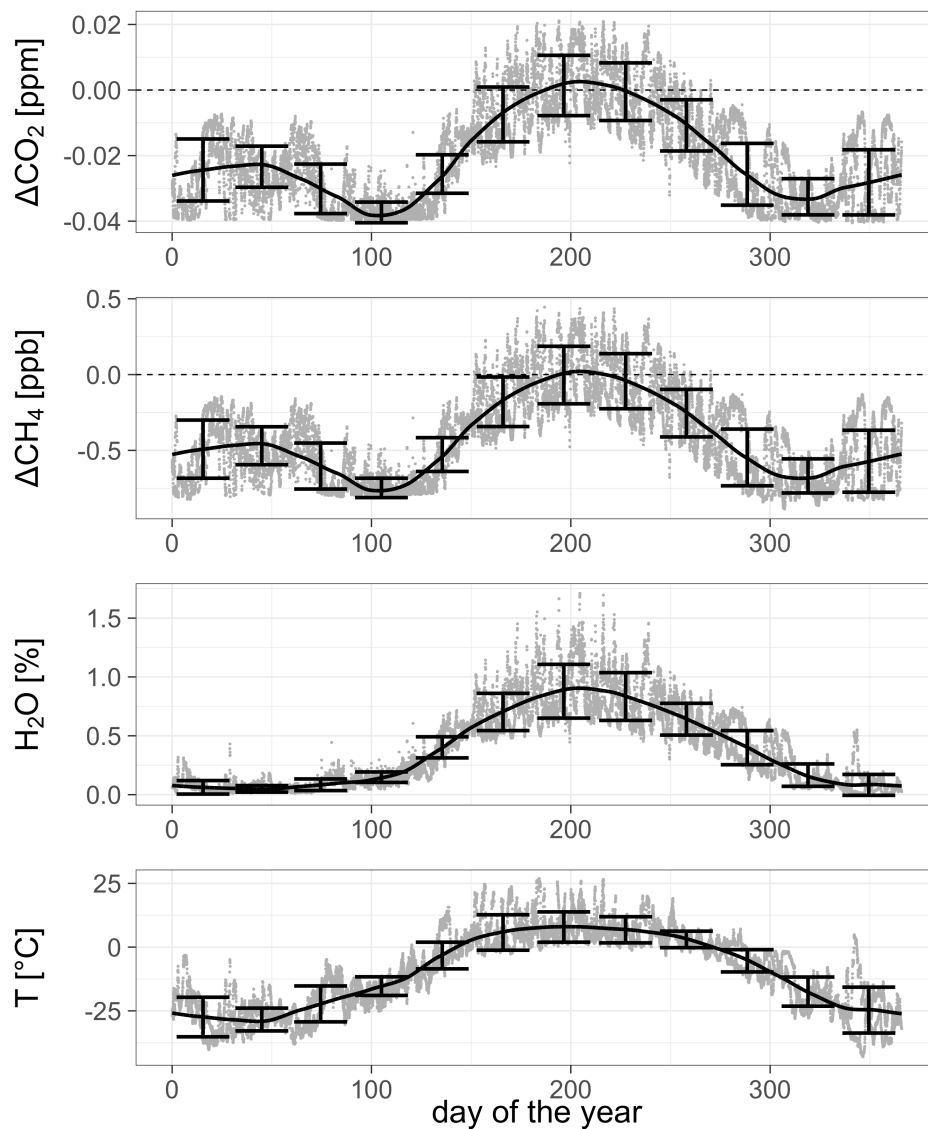


Fig. 6: Difference between the traditional and the improved water correction of Ambarchik data for 2015 and 2016. Dots: hourly averages of the air inlet at 27 m, line: smoothed data, error bars: monthly averages and standard deviation. Water vapor content and ambient temperature are plotted for reference.

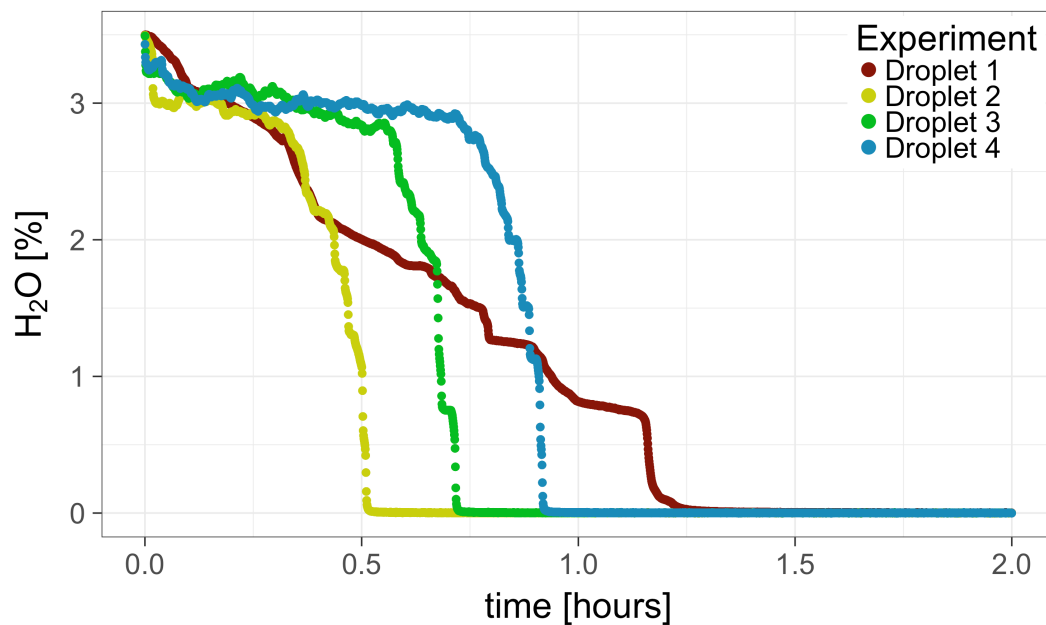


Fig. 7: Temporal progression of water vapor content during the droplet experiments after the drop below 3.5 % H₂O. To illustrate the effect of fast water vapor changes on pressure, fast water vapor variations have not been filtered out for this plot.

5

10

15

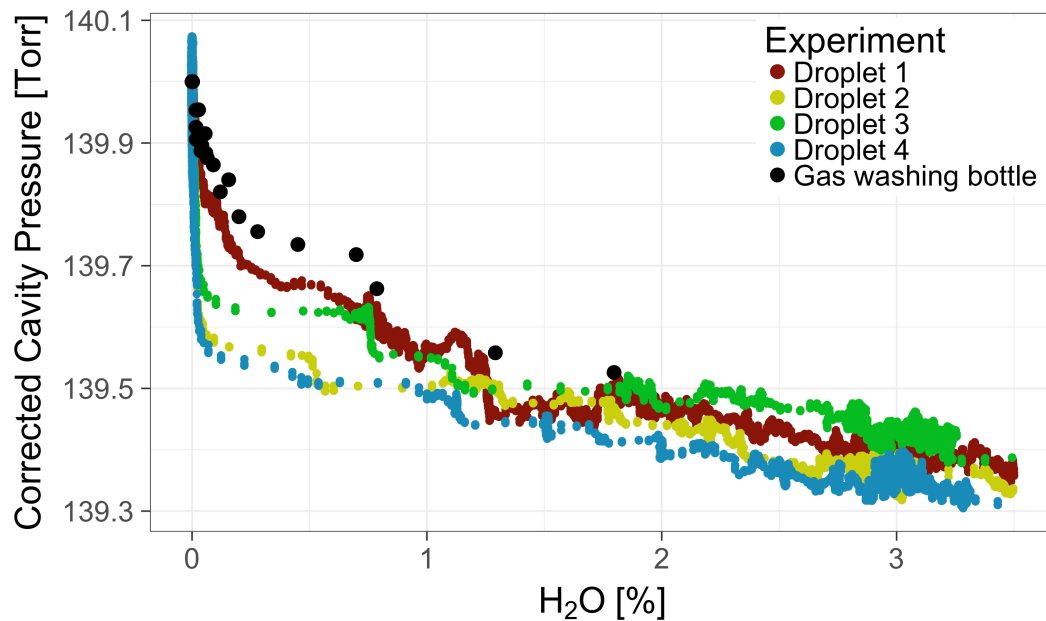


Fig. 8: Cavity pressure during four droplet experiments and one gas washing bottle experiment with Picarro #1. To illustrate the effect of fast water vapor changes on pressure, fast water vapor variations have not been filtered out for this plot.

5

10

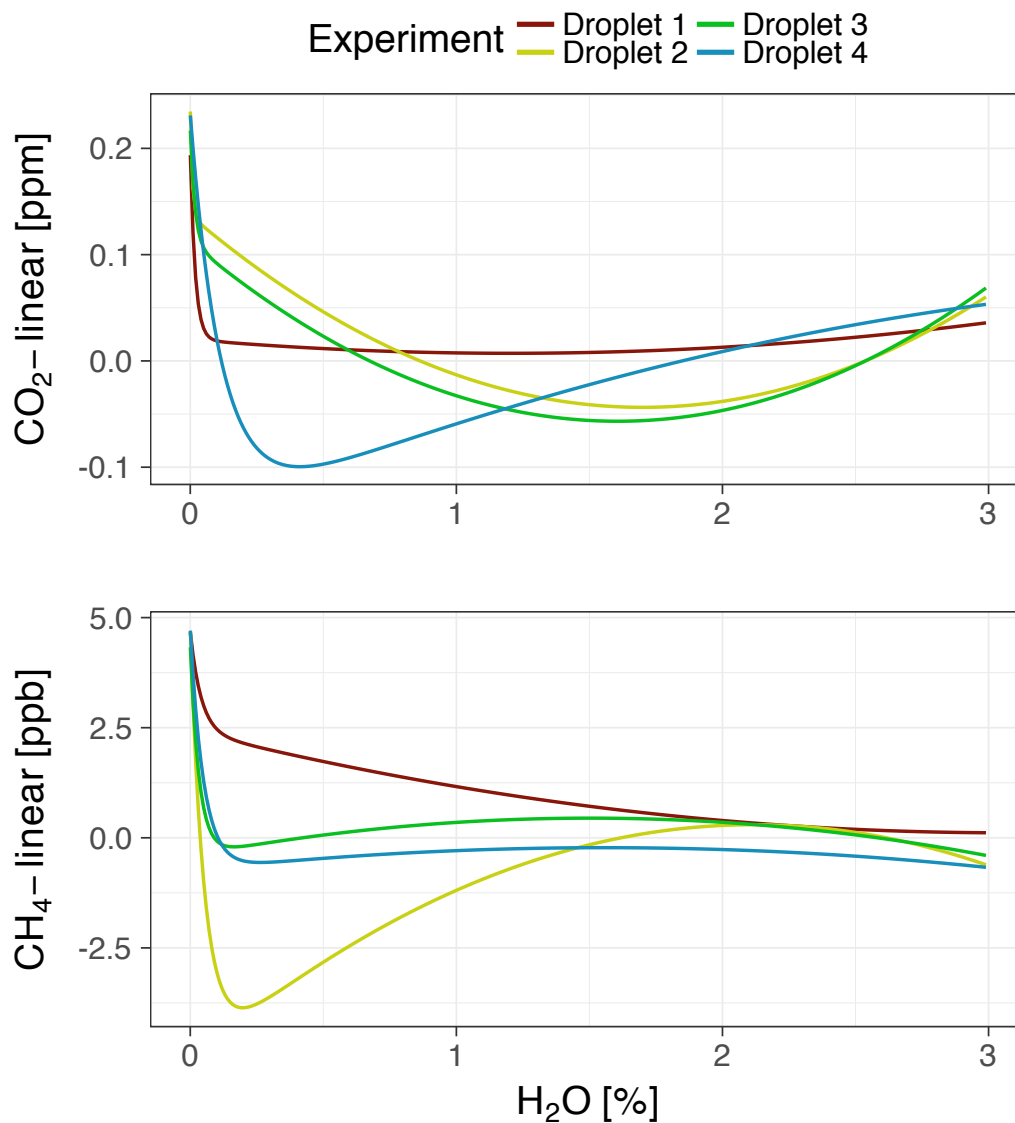


Fig. 9: Fit functions to data from four droplet experiments with Picarro #1. To emphasize differences, a common linear component has been subtracted from the fit functions. In these fits, the pressure bend position h_p has been fit to the trace gas data.